

Foundation and the National Institutes of Health. The rest of the authors declare that they have no relevant conflicts of interest.

## REFERENCES

1. Popov TA. Human exhaled breath analysis. *Ann Allergy Asthma Immunol* 2011; 106:451-6.
2. Tomasiak-Lozowska MM, Zietkowski Z, Przeslaw K, Tomasiak M, Skiepkowski R, Bodzenta-Lukaszyk A. Inflammatory markers and acid-base equilibrium in exhaled breath condensate of stable and unstable asthma patients. *Int Arch Allergy Immunol* 2012;159:121-9.
3. Zhang J, Zhao H, Gao Y, Zhang W. Secretory miRNAs as novel cancer biomarkers. *Biochim Biophys Acta* 2012;1826:32-43.
4. Chen RF, Huang HC, Ou CY, Hsu TY, Chuang H, Chang JC, et al. MicroRNA-21 expression in neonatal blood associated with antenatal immunoglobulin E production and development of allergic rhinitis. *Clin Exp Allergy* 2010;40:1482-90.
5. Chiba Y, Misawa M. MicroRNAs and their therapeutic potential for human diseases: MiR-133a and bronchial smooth muscle hyperresponsiveness in asthma. *J Pharmacol Sci* 2010;114:264-8.
6. Collison A, Herbert C, Siegle JS, Mattes J, Foster PS, Kumar RK. Altered expression of microRNA in the airway wall in chronic asthma: miR-126 as a potential therapeutic target. *BMC Pulm Med* 2011;11:29.
7. Kumar M, Ahmad T, Sharma A, Mabalirajan U, Kulshreshtha A, Agrawal A, et al. Let-7 microRNA-mediated regulation of IL-13 and allergic airway inflammation. *J Allergy Clin Immunol* 2011;128:1077-85.
8. Mattes J, Collison A, Plank M, Phipps S, Foster PS. Antagonism of microRNA-126 suppresses the effector function of TH2 cells and the development of allergic airways disease. *Proc Natl Acad Sci U S A* 2009; 106:18704-9.

Available online April 28, 2013.  
<http://dx.doi.org/10.1016/j.jaci.2013.03.006>

## Exosome-enclosed microRNAs in exhaled breath hold potential for biomarker discovery in patients with pulmonary diseases

### To the Editor:

MicroRNAs (miRNAs) are small noncoding RNAs of 22 to 25 nucleotides in length that act through an RNA-induced silencing complex to posttranscriptionally regulate mRNAs that contain complementary sequences. Highly stable circulating miRNAs are found in biological fluids and are potential biomarkers.<sup>1,2</sup> These are often enclosed in small secretory membrane vesicles called exosomes, which permit transfer of miRNA between cells.<sup>3</sup> Exhaled breath condensate (EBC), which can be obtained noninvasively and conveniently and is representative of the airway lining fluid, could be an ideal substrate for discovery of pulmonary disease biomarkers.<sup>4-6</sup> For the first time, we report that miRNAs can be reliably detected in EBC by using quantitative PCR analysis and are suitable as biomarkers.

Briefly, EBC was collected over 10 minutes with an RTube (Respiratory Research, Austin, Tex), as per the recommended protocol. RNA was extracted with the miRvana small RNA extraction kit (Ambion, Invitrogen, Carlsbad, Calif) from vacuum-dried and concentrated EBC samples. Equal amounts of quantitated RNA (Nanodrop; Thermo Fisher, Uppsala, Sweden) were used to prepare the cDNA by using miRNome cDNA synthesis kits (System Biosciences, Mountain View, Calif), and finally, 5  $\mu$ L of the cDNA was used to perform quantitative PCR (LightCycler 480II; Roche, Mannheim, Germany). Sample input and processing were tightly standardized, and data variability was acceptable, even without any normalization (see the **Methods** section in this article's Online Repository at [www.jacionline.org](http://www.jacionline.org)). A quantitative PCR cycle threshold (Ct) cutoff of 18 or greater and 35 or less was used to focus on those species of miRNAs that have reliable expression levels. Institutional committees approved all research protocols.

To determine the miRNA profile of EBC and its variation across age and disease, we measured the full miRNome of approximately 1000 miRNAs for 10 subjects with asthma and 10 healthy subjects with no known disease. We found that using a minimum cut-off of at least 5 positive samples (from 20 total samples), 643 miRNAs were detectable in EBC with acceptable intersample variability (SD, 1-2 Ct for most miRNAs; see **Table E1** in this article's Online Repository at [www.jacionline.org](http://www.jacionline.org)).

Highly abundant miRNAs in EBC, such as hsa-let7, hsa-miR-181c, and hsa-miR-1307, have been previously found to be abundant in lung tissue and were similar across most subjects. The EBC miRNA profile of asthmatic patients was generally similar to that of healthy subjects, and no miRNA crossed the multiple-comparison adjusted significance threshold of a *P* value of less than .0001. However, 11 miRNAs were somewhat differently expressed in asthmatic patients compared with healthy subjects based on a combination of fold differences in expression and detection in a majority of samples to increase reliability (**Fig 1, A**, and see **Table E1** for details and statistics). Of these, at least 3 (hsa-miR-574-5p, hsa-miR-516a-5p, and hsa-miR-421) are previously known to be involved in asthma-, allergy-, and inflammation-related pathways.<sup>7</sup> Results of a preliminary validation study with different stem-loop primers for hsa-miR-2861, hsa-miR-574-5p, and hsa-miR-556-5p in human lung biopsy samples (*n* = 2 each) and additional EBC samples (*n* = 6 each) were consistent with the initial findings. Pooling the validation samples with the discovery set led to increased statistical confidence (95% CI ratios for asthmatic patients/healthy subjects in pooled samples: hsa-miR-2861, 1.2-3.2; hsa-miR-574-5p, 1.3-2.3; and hsa-miR-556-5p, 0.3-0.5), but only hsa-miR-556-5p met the significance criteria (*P* < .0001). Further testing is needed to determine clinical utility.

To test whether these miRNA signatures reflect asthma, we additionally measured their levels in EBC from 9 patients with pulmonary tuberculosis (**Fig 1, B**, and see **Table E1**). Seven of the 11 differently expressed miRNAs in asthmatic patients were also correspondingly altered in patients with tuberculosis, although to a much higher degree. These changes were highly statistically significant, confirming that these miRNAs do reflect disease but are not specific to asthma, possibly reflecting general inflammatory changes or epithelial damage. Interestingly, hsa-miR-4256 and hsa-miR-453 were significantly altered in opposite directions in asthmatic patients and patients with tuberculosis in comparison with healthy subjects and seem more specific. Interestingly, hsa-miR-345, which is downregulated in lungs by cigarette smoke exposure,<sup>8</sup> was also specifically downregulated (*P* = .001) in asthmatic patients after applying a normalization algorithm for samples in which the normalization strategy is debatable (see the **Methods** section in this article's Online Repository). Although our study focuses on asthma with tuberculosis as a control, it would be interesting to see whether other pulmonary infections and tuberculosis can be distinguished by EBC miRNA.

Because miRNAs appeared to be highly stable in EBC, unlike mRNA, we further hypothesized that miRNAs in EBC might be enclosed within exosomes. Therefore the presence of exosomes was probed in concentrated EBC samples. Latex beads (singlets; see **Fig E1, A**, in this article's Online Repository at [www.jacionline.org](http://www.jacionline.org)) coated with anti-CD63 antibody (exosome specific; see **Fig E1, B**) were used to bind exosomes and pelleted to separate the exosomal fraction. We found that exosomes are present in EBC and contain the majority of the miRNA content (**Fig**

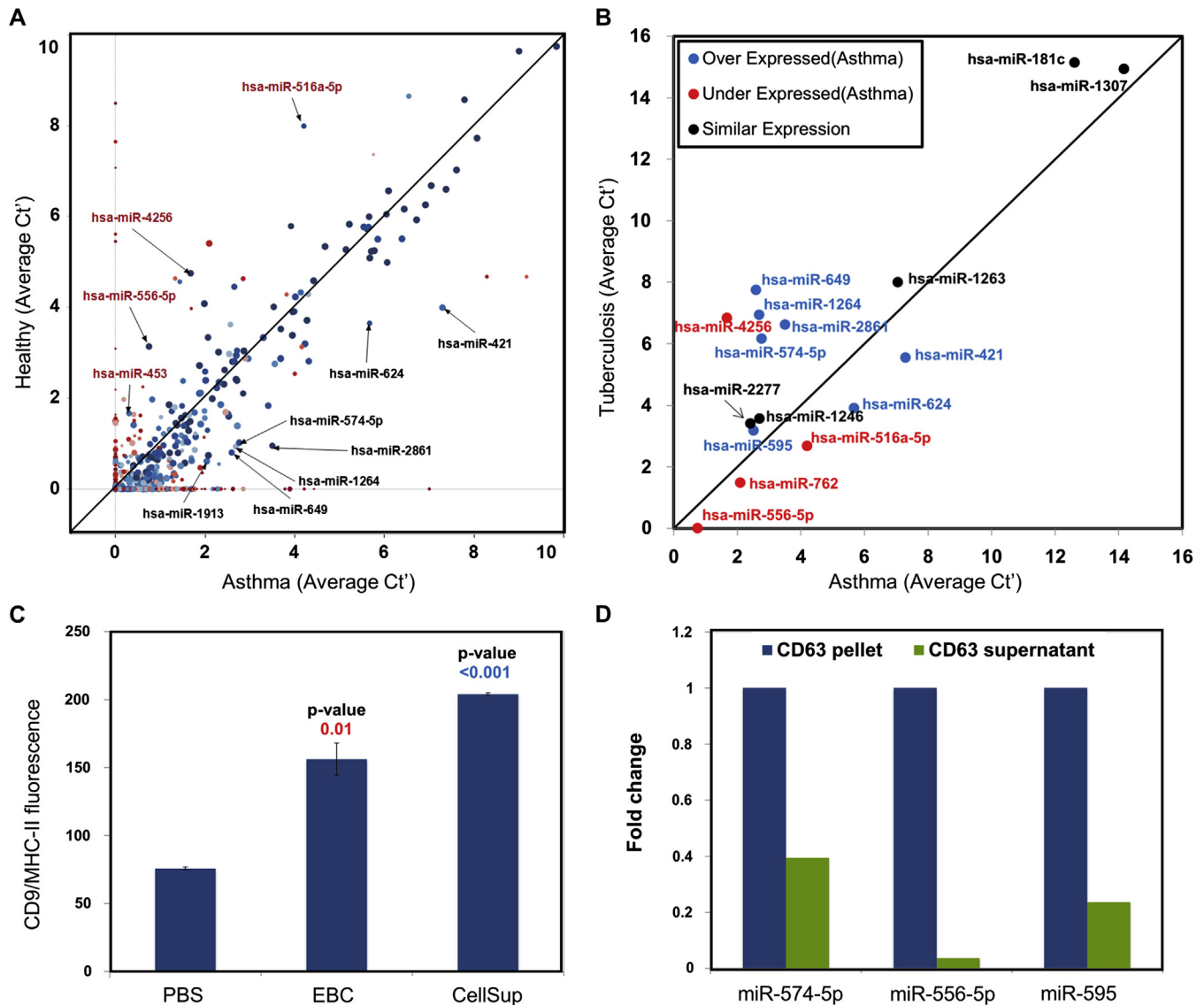


**FIG 1.** EBC miRNAs are potential biomarkers and contained in exosomes. **A**, Correlation bubble plot of miRNA expression between the healthy and asthma groups. Color (red to blue) and size (small to large) denote sample counts in the asthma and healthy groups, respectively. miRNAs with high sample counts (large blue circles) were selected from the regions away from the unity line with a fold change of 2 or greater (axes truncated; see the extended legend for Fig 1 in this article's Online Repository at [www.jacionline.org](http://www.jacionline.org) for details). **B**, Scatter plot of miRNA expression between the asthma and tuberculosis groups. Red and blue circles indicate miRNAs overexpressed and underexpressed in asthmatic patients with respect to healthy subjects, respectively. Black circles indicate miRNAs with no differential expression in the 3 groups. **C**, Fluorescence of CD9/MHC-II measured by means of fluorescence-activated cell sorting confirming that EBC contains exosomes. CellSup, Cell culture supernatant (positive control). PBS is the negative saline control. **D**, Relative miRNA content of the exosome (CD63 pellet) and nonexosome (supernatant), confirming that exosomes contain the majority of miRNAs.

1, C and D). This is significant for 2 reasons. First, it is likely that the EBC miRNome reflects ongoing biological processes because exosome secretion and exosome contents are highly regulated.<sup>9</sup> Second, this ensures that measurement of the EBC miRNome will be a robust strategy that does not require extreme care during sample storage and transport. The tissue source of exosomes in EBC remains to be characterized.

Because exosomes are known to mediate miRNA targeting of distant cells, we speculated whether miRNA content of exhaled breath, being contained in exosomes, might target epithelial

cells of the airway. Therefore we obtained scrapes of the posterior nasal respiratory epithelial cells in a separate group of subjects, examined gene expression profiles, and compared these with the targets of the miRNAs associated with asthma (see Fig E2 and Table E2 in this article's Online Repository at [www.jacionline.org](http://www.jacionline.org)). There were clear differences between gene expression patterns in subjects with or without asthma (Fig 2), with the asthma pathway predicted to be of high importance (see Fig E3 in this article's Online Repository at [www.jacionline.org](http://www.jacionline.org)). Notably, predicted mRNA targets of the

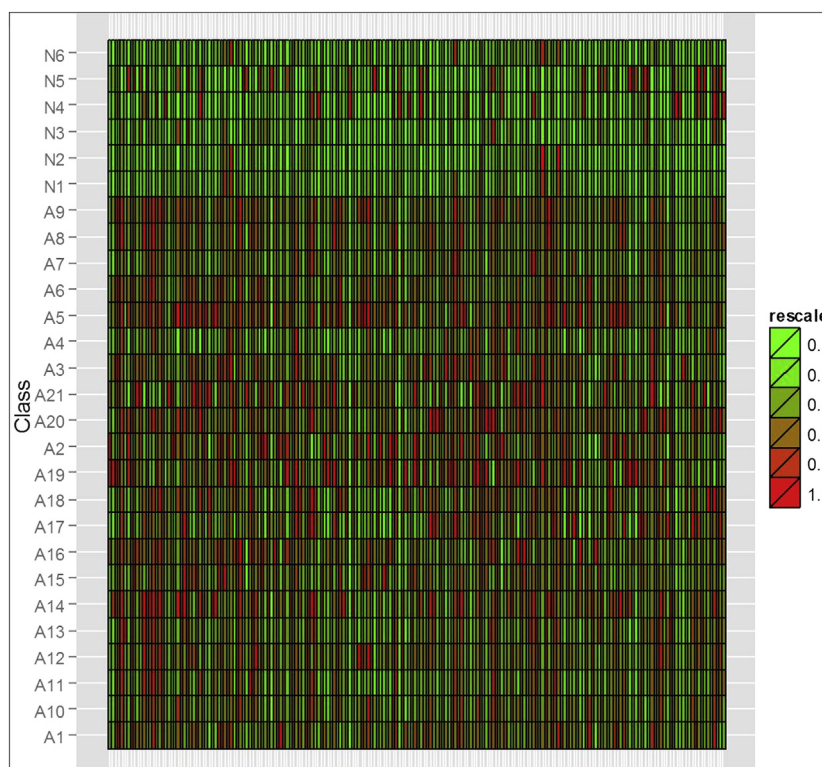


**FIG 2.** Heat map showing differential expression of genes (*x-axis*, column) in nasal scrapings across 6 healthy subjects (*N*) and 21 asthmatic patients (*A*). The gene expression values were rescaled to lie between an arbitrarily selected range of 0 to 1. The numeric values were shown as colors indicating the relative expression of genes, with red being the most expressed and green being the least expressed.

upregulated miRNAs were downregulated in nasal epithelium (eg, *SLCO2A1* and *PAX7*) and vice versa (eg, *HLA-DPBI* and *NAV2*). However, this is not direct proof of any effect of the exosomal miRNAs in breath and epithelial mRNAs and is only hypothesis generating.

In summary, we found that miRNAs are present in EBC, mostly in a stable membrane-enclosed form. We also provide proof of principle that lung disease can lead to alteration in the EBC miRNome and that the study of miRNAs in EBC is a fertile ground for clinical biomarker discovery, as well as understanding disease.

We thank Gopal Gunanathan, Dr Naveen Bhatraju, and Parul Chauhan for their assistance.

Anirban Sinha, MSc<sup>a</sup>  
Amit Kumar Yadav, MSc<sup>a</sup>  
Samarpana Chakraborty, MSc<sup>a</sup>  
S. K. Kabra, MD<sup>b</sup>  
R. Lodha, MD<sup>b</sup>  
Manish Kumar, MSc<sup>a</sup>  
Ankur Kulshreshtha, MTech<sup>a</sup>  
Tavpritesh Sethi, MBBS<sup>a</sup>  
Rajesh Pandey, PhD<sup>a</sup>  
Gaurav Malik, BTech<sup>a</sup>  
Saurabh Laddha, MSc<sup>a</sup>  
Arijit Mukhopadhyay, PhD<sup>a</sup>  
Debasis Dash, PhD<sup>a</sup>  
Balaram Ghosh, PhD<sup>a</sup>  
Anurag Agrawal, MD, PhD<sup>a</sup>

From <sup>a</sup>CSIR-Institute of Genomics and Integrative Biology and <sup>b</sup>the All India Institute of Medical Science, New Delhi, India. E-mail: a.agrawal@igib.res.in.

Supported by a Grant-in-Aid for Scientific Research from the Council of Scientific and Industrial research, India, through grant MLP-5502 and the Department of Science and Technology, India, through Swarnajayanti Fellowship.

Disclosure of potential conflict of interest: The authors declare that they have no relevant conflicts of interest.

#### REFERENCES

1. Cortez MA, Bueso-Ramos C, Ferdin J, Lopez-Berestein G, Sood AK, Calin GA. MicroRNAs in body fluids—the mix of hormones and biomarkers. *Nat Rev Clin Oncol* 2011;8:467-77.
2. Jung M, Schaefer A, Steiner I, Kempkensteffen C, Stephan C, Erbersdobler A, et al. Robust microRNA stability in degraded RNA preparations from human tissue and cell samples. *Clin Chem* 2010;56:998-1006.
3. Valadi H, Ekstrom K, Bossios A, Sjostrand M, Lee JJ, Lotvall JO. Exosome-mediated transfer of mRNAs and microRNAs is a novel mechanism of genetic exchange between cells. *Nat Cell Biol* 2007;9:654-9.
4. Sinha A, Krishnan V, Sethi T, Roy S, Ghosh B, Lodha R, et al. Metabolomic signatures in nuclear magnetic resonance spectra of exhaled breath condensate identify asthma. *Eur Respir J* 2012;39:500-2.
5. Horvath I, Hunt J, Barnes PJ, Alving K, Antczak A, Baraldi E, et al. Exhaled breath condensate: methodological recommendations and unresolved questions. *Eur Respir J* 2005;26:523-48.
6. Bloemen K, Van Den Heuvel R, Govarts E, Hooyberghs J, Nelen V, Witters E, et al. A new approach to study exhaled proteins as potential biomarkers for asthma. *Clin Exp Allergy* 2011;41:346-56.
7. Garbacki N, Di Valentin E, Huynh-Thu VA, Geurts P, Irrthum A, Crahay C, et al. MicroRNAs profiling in murine models of acute and chronic asthma: a relationship with mRNAs targets. *PLoS One* 2011;6:e16509.
8. Izzotti A, Larghero P, Longobardi M, Cartiglia C, Camoirano A, Steele VE, et al. Dose-responsiveness and persistence of microRNA expression alterations induced by cigarette smoke in mouse lung. *Mutat Res* 2011; 717:9-16.

9. Keller S, Sanderson MP, Stoek A, Altevogt P. Exosomes: from biogenesis and secretion to biological function. *Immunol Lett* 2006;107:102-8.

Available online May 14, 2013.  
<http://dx.doi.org/10.1016/j.jaci.2013.03.035>

## Severe phenotype of severe combined immunodeficiency caused by adenosine deaminase deficiency in a patient with a homozygous mutation due to uniparental disomy

To the Editor:

Severe combined immunodeficiency caused by adenosine deaminase deficiency (ADA-SCID) commonly presents with a phenotype consisting of life-threatening infections, chronic persistent diarrhea, and failure to thrive in the first months of life.<sup>1</sup> In patients with ADA-SCID, toxic metabolites will destroy the lymphocytes and lead to absent or decreased numbers of B, T, and natural killer cells. Patients with ADA-SCID not only have an immunodeficiency but also other organs might be affected if increased concentrations of the metabolite persist.<sup>2</sup> ADA-SCID is autosomal recessively inherited through mutations in the *ADA* gene, which is located on chromosome 20q13.12.

We present a patient with a severe phenotype of ADA-SCID. She was the second child of healthy unrelated Dutch parents and prematurely born (35<sup>+2</sup> weeks gestation) by means of emergency cesarean section because of lack of fetal movement and abnormal heart rate. Apgar scores were 6/9/9. Immediately after birth, dysmorphic facial features (including a broad nasal tip, epicanthal folds, large low-set ears, and microretrognathia), microcephaly, erythroderma, and thermolability were noted. A skin biopsy specimen did not show any indicative abnormalities. During the neonatal period, she had a urinary tract infection with *Klebsiella* species, paronychia of the fingers on both hands, and multiple episodes of cellulitis associated with intravenous catheters for which she received intravenous antibiotic treatments and surgical incisions. She had hypotonia, absent reflexes, blindness and deafness, and an abnormal breathing pattern.

Because of the erythroderma and infectious problems combined with lymphocytopenia in peripheral blood, a primary immunodeficiency was suspected. Flow cytometry showed no B, T, or natural killer cells ( $<0.02 \times 10^9$  cells/L per subpopulation). IgA and IgM levels were not measurable (both  $<0.07$  g/L), and the concentration of IgG decreased over time (2.9 g/L on day 26). The diagnosis of severe combined immunodeficiency (SCID) was made. Biochemical analysis demonstrated a complete deficiency of adenosine deaminase (ADA) activity in the erythrocytes.

At day 26, she had respiratory insufficiency requiring artificial ventilation. She had a lower airway infection and symptoms of acute respiratory distress syndrome. After 4 days of intensive treatment and artificial ventilation, further medical treatment was withdrawn because of the very limited treatment options, the prognosis of the ADA-SCID itself, and the irreversible neurologic condition.

Sequence analysis of our patient demonstrated homozygosity for a 5-bp deletion (c.956\_960delAAGAG) in exon 10 of the *ADA* gene. This frameshift mutation leads to a premature stop codon, resulting in a truncated protein. Analysis of the parental DNA showed that only the father was a heterozygous carrier for this deletion. Considering the autosomal recessive inheritance of ADA-SCID, this did not match with the homozygous occurrence in our patient. 250K Nsp SNP Array (Affymetrix, Santa Clara, Calif)

analysis of the patient-parent trio was performed to examine the scenario of either a maternal deletion within the *ADA* gene or a paternal uniparental disomy of chromosome 20 (UPD[20]). The patient data showed a large approximately 50-Mb region of homozygosity on chromosome 20 (p13q13.2 from 0.85 to 51.71 Mb) encompassing hundreds of genes, including the *ADA* gene (located at approximately 42.25 Mb). On the basis of the single nucleotide polymorphism data, we could determine that both entire chromosomes 20 of our patient were of paternal origin. They contained 2 terminal heterodisomic regions (that contain the 2 different paternal alleles) and an isodisomic region (containing 2 identical paternal alleles), leading to homozygosity of the pathogenic 5-bp deletion in *ADA*. This phenomenon is called a UPD and is the result of a rescue of trisomy 20 in very early embryonic development (Fig 1). UPD is a rare causative mechanism of autosomal recessive disease and has never been described for patients with ADA-SCID. Understanding the mechanism of inheritance is very important, especially for determining the risk of recurrence.

The mutation has been described before in patients with ADA-SCID.<sup>3-5</sup> Because our patient has a homozygous mutation with a truncated nonfunctional protein, a severe phenotype can be expected.<sup>6</sup>

Because the molecular defect in patients with ADA-SCID is not only present in hematopoietic cells, metabolic problems can also occur in other tissues.<sup>2</sup> Our patient demonstrated dysmorphic features and erythroderma. Erythroderma, as seen in patients with Omenn syndrome, has been described before in patients with ADA-SCID with residual ADA activity.<sup>7</sup> Activated oligoclonal T cells are thought to be the cause of erythroderma in patients with Omenn syndrome, but these cells were not detected in our patient. On the other hand, the erythroderma might reflect an aberrant inflammatory condition associated with SCID caused by multiple genetic defects.<sup>8</sup>

Whether the dysmorphic features result from the specific deletion is unclear. One possibility is that the additional features are caused by the UPD(20) for chromosome 20 itself. Several patients with UPD(20) have been described and share features like microcephaly, prenatal and postnatal growth retardation, and mild dysmorphism.<sup>9</sup> Another possibility is the presence of a mosaicism for trisomy 20 as a "leftover" of the rescue mechanism very early in life. Full trisomy 20 has not been described in a live-born patient and is expected to be incompatible with life. Trisomy 20 mosaicism has rarely been described and is usually associated with a mild phenotype. A CytoScan HD array (Affymetrix) did not show any sign of trisomy 20 in the DNA derived from a skin biopsy specimen, making this possibility highly unlikely.<sup>10</sup> Other more sensitive techniques to detect mosaicism, such as fluorescence *in situ* hybridization analysis, could not be performed because no suitable material was available. A final possibility is homozygosity for a mutation in one of the other genes ( $>100$ ) in the UPD region.

The recurrence risk of UPD without chromosomal disturbances in parents is low ( $<1\%$ ). Because the recurrence risk would be 25% when both parents are a carrier of the mutation, this indicates how important understanding the mechanism of inheritance is for correct counseling of the parents.

Joyce Geelen, PhD<sup>a</sup>

Rolph Pfundt, PhD<sup>b</sup>

Judith Meijer, BASc<sup>c</sup>

Frans W. Verheijen, PhD<sup>d</sup>

Andre B. P. van Kuilenburg, PhD<sup>e</sup>

## METHODS

### EBC

Exhaled breath was collected with the RTube (Respiratory Research) over a 10-minute protocol, as per recommendations. It was concentrated for 3 hours by using Eppendorf Concentrator Plus (Eppendorf, Hamburg, Germany). The samples were then stored at  $-80^{\circ}\text{C}$ .

### RNA isolation

RNA was isolated by using the miRvana small RNA extraction kit (Ambion), as per the manufacturer's protocol with minor modifications, because exhaled breath is extremely dilute. The isolated RNA was quantitated with the Nanodrop 1000 Spectrophotometer (Thermo Scientific).

### cDNA synthesis and real-time PCR analysis

cDNA was prepared with 60 ng of RNA by using the QuantiMir cDNA synthesis kit (System Biosciences), and finally, 5  $\mu\text{L}$  of cDNA was used as a template for real-time analysis by using the miRNome real-time quantitative PCR setup (System Biosciences). The instrument used was the Light Cycler 480 II (Roche).

Quantitative PCR was used to quantify the variations in miRNA content of EBC. The PCR-amplified product was detected with SYBR Green dye, and the increase in SYBR Green fluorescence was measured in real time. In brief, 5  $\mu\text{L}$  of cDNA sample was mixed with SYBR Green I master mix per the manufacturer's protocol (System Biosciences), and the quantitative PCR reaction was carried out in a pre-primer-coated 384-well plate using the Light cycler 480II (Roche).

The thermal cycles were as follows: (1) preincubation—cycles, 1; temperature,  $95^{\circ}\text{C}/5$  minutes; (2) amplification—cycles, 45; temperature/time,  $95^{\circ}\text{C}/10$  seconds,  $60^{\circ}\text{C}/10$  seconds, and  $72^{\circ}\text{C}/10$  seconds; (3) melting curve—cycles, 1; temperature/time,  $95^{\circ}\text{C}/5$  seconds,  $65^{\circ}\text{C}/1$  minute; and (4) cooling—cycles, 1; temperature/time,  $40^{\circ}\text{C}/30$  seconds.

The Ct value for each amplification can be defined as the cycle in which the fluorescence signal crosses a threshold level that is above any background fluctuations in fluorescence. This value is associated with the initial amount of DNA present in the sample and is inversely proportional to the expression level of the gene. For more intuitive representation in XY plots, Ct was converted to Ct' (35-Ct), such that a higher Ct' value means higher expression of miRNAs.

### Analyses of miRNome data

As a primary filter, all Ct values of 18 or less and 35 or greater were excluded. Each Ct value was then transformed by using the following formula:

$$Ct' = 35 - Ct.$$

Ct' values from all 10 samples from each group were collated. Average Ct' values were calculated for both the groups. Fold change (FC) for every miRNA was calculated as follows:

$$FC = 2^{\Delta Ct'},$$

where  $\Delta Ct'$  is defined as follows:

$$|\text{Average } Ct'(\text{Healthy}) - \text{Average } Ct'(\text{Asthma})|.$$

These calculations and collations were done with a perl program.

### Normalization of miRNome data

The default analysis was done without normalization because it was not known which miRNA was stably expressed in EBC. XY plots of miRNA expression between groups followed the line of unity, suggesting lack of any systematic errors that could have introduced a bias. However, to assess the potential effect of variations in input RNA, we attempted to discover a suitable miRNA for normalizing EBC and performed a revised analysis. Using a code written in perl, the normalizing miRNA (present in all samples and with least

SD) was identified as hsa-miR-575. Next, the normalizing miRNA's Ct value in a particular sample was used to normalize every other Ct value for that sample by using the following formula:

$$Ct'_{ij} = NCt_i - Ct_{ij},$$

where  $Ct'_{ij}$  is defined as the normalized value of Ct for *i*th sample's *j*th miRNA;  $NCt_i$  is defined as the normalizing miRNA's Ct value for the *i*th sample, which is used for normalizing other Ct values for that particular *i*th sample; and  $Ct_{ij}$  is defined as the Ct value for the *i*th sample's *j*th miRNA.

No major changes were made to the analysis after normalization, with 9 of 11 prioritized miRNAs being minimally changed. There was a marked increase in the significance of 2 miRNAs (miR-453 to  $P = .001$  and miR-345 to  $P = .002$ ). However, because the validity of miR-575 as a stably expressed miRNA in EBC is unclear at this time, the unadjusted values are reported in Table E1.

### Bioinformatic analysis

Gene targets were predicted for the most regulated (both upregulated and downregulated) miRNAs by using the entire human genome data, with a consensus of TargetScan and miRanda software. Because it is likely that miRNAs target multiple genes along related pathways, the target gene list was analyzed for enriched pathways by using the Database for Annotation, Visualization and Integrated Discovery (DAVID; Fig E2).

### Validation of miRNome results

The top 2 primers from the upregulated batch (hsa-miR-574-5p and hsa-miR-2861) and 1 primer from the downregulated batch (hsa-miR-556-5p) having a stem-loop design were selected to validate the miRNome results in EBC of different patients ( $n = 6$  each) by using real-time PCR analysis.

In a preliminary study the same miRNAs were also found differentially expressed in human lung biopsy samples from patients and healthy subjects ( $n = 2$  each), which is consistent with our findings in EBC.

### Detecting the presence of exosomes in EBC samples

Concentrated EBC was incubated with anti-CD63 antibody-coated beads and kept overnight on a rotary shaker at 50 rpm. The beads coated with exosomes were saturated with 2% BSA for 30 minutes, followed by incubation with anti-CD81/CD9/MHC-II antibody (BD Biosciences, San Jose, Calif) at 1:100 dilution for 30 minutes in the dark. Samples were acquired on a BD FACSCalibur by gating onto single beads. Five thousand events were counted for each sample. PBS was used as a negative control, whereas THP-1 cell culture supernatant was used as a positive control.

In a separate experiment the effectiveness of the beads in pulling down the exosomes was confirmed by incubating the beads with cell culture supernatant from THP-1 cells and then detecting the associated proteins Tsg-101 and Alix in the pelleted fraction by means of Western blotting with the antibody against these 2 proteins (Fig E1, A).

### Extraction and detection of miRNA from the bead-bound exosome-enriched fraction in EBC

Exhaled breath samples from different patients collected at multiple times were pooled and concentrated, as mentioned previously. They were incubated with anti-CD63 antibody-coated beads overnight in an Eppendorf rotor mixer at  $4^{\circ}\text{C}$ . Next, the sample was centrifuged at  $10,000g$  for 30 minutes. Pellets and supernatants were separated, and miRNA was extracted from both fractions, followed by cDNA synthesis with the Revert aid H minus first-strand cDNA synthesis kit (Fermentas Life Sciences, Thermo Scientific).

Real-time PCR analysis was done with primers of miRNA selected from the most differentially regulated list (hsa-miR-574-5p, hsa-miR-595, and hsa-miR-556-5p).

### Isolation of RNA from nasal epithelial scrapings and subsequent cDNA microarray analysis

Nasal epithelial cells were scraped off 10 times from the inferior turbinate of the nose of subjects, followed by immediate storage in RLT buffer. RNA was isolated with the RNeasy Mini kit 50 (Qiagen, Hilden, Germany), quantitated with Nanodrop, and stored at  $-80^{\circ}\text{C}$ .

Samples from asthmatics (without allergic rhinitis) and control subjects were selected based on RNA integrity determined by using gel electrophoresis and concentrations. These samples were subsequently converted to cDNA, followed by microarray experiment on the Illumina Platform (Illumina, San Diego, Calif). The microarray data were analyzed by using the GenomeStudio Platform (Illumina) and examined for differentially regulated genes. The differentially regulated genes were fed into pathway enrichment tools, such as pathway express and DAVID, to look for enriched pathways related to our study (Fig E3).

**Fig 1.** Figs 1, *A* and *B*, are plotted by using average  $\text{Ct}'$  values for the corresponding group (healthy subjects, asthmatic patients, or patients with

tuberculosis). Fig 1, *A*, shows the average  $\text{Ct}'$  values for asthmatic patients and healthy subjects, whereas Fig 1, *B*, shows the average  $\text{Ct}'$  values for asthmatic patients and patients with tuberculosis. These average  $\text{Ct}'$  values are used to denote expression levels of miRNAs. In Fig 1, *A*, the underexpressed miRNAs are found to be above the diagonal line, where the size of the bubble is large (high sample count in healthy subjects) and blue in color (high sample counts in asthmatic patients). Similarly, the overexpressed miRNAs are seen below the diagonal line with larger, blue-colored circles. The axes have been truncated for the sake of clarity. The miRNAs removed by means of truncation are not differentially expressed (either low or high). Fig 1, *B*, shows the scatter plot of average  $\text{Ct}'$  values compared between asthmatic patients and patients with tuberculosis. The overexpressed and underexpressed miRNAs in asthmatic patients are with respect to the healthy samples. "Similar expression" miRNAs are denoted with respect to mutual comparison of the asthma and tuberculosis groups. This is done to bring out the similarities and differences of underexpressed and overexpressed miRNAs with respect to tuberculosis.

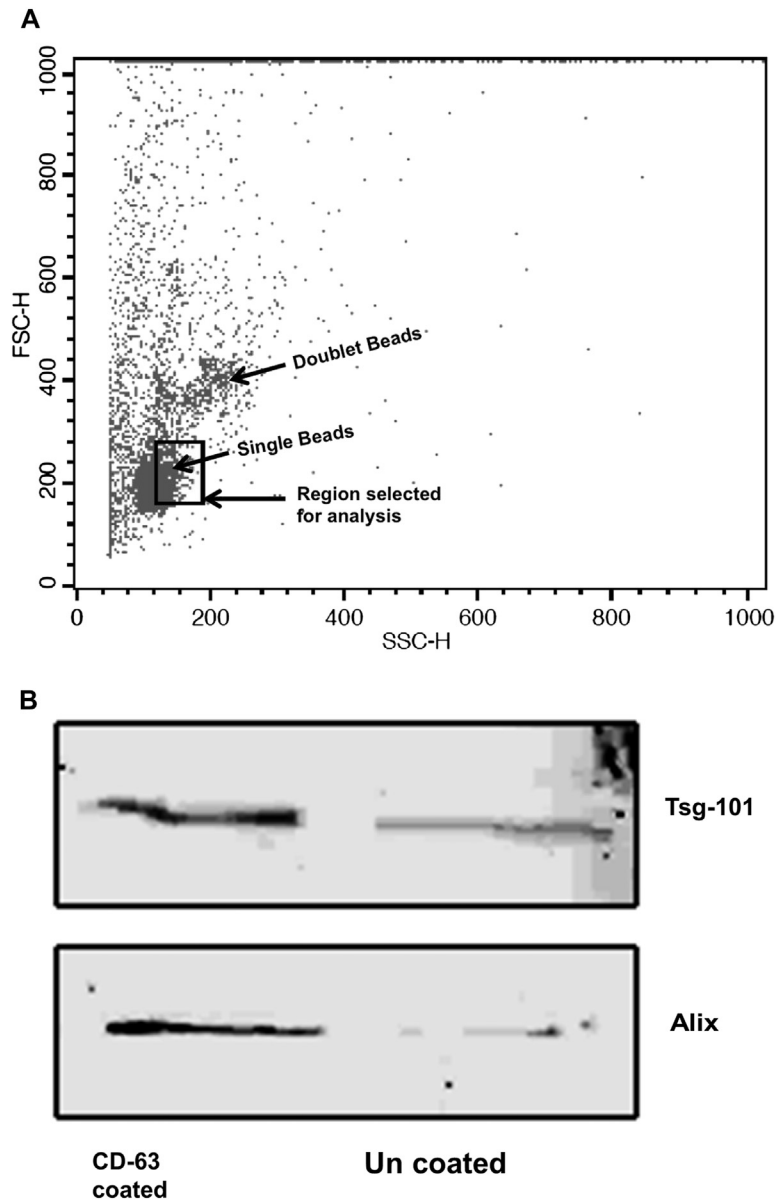


**FIG E1.** **A**, The forward scatter (*FSC*)–side scatter (*SSC*) plot shows the bead selection for detection of bead-bound exosomes. The selected region marks the region for further analysis across various groups. **B**, Exosomal marker proteins (Tsg-101 and Alix) are seen in anti-CD63 antibody-coated beads in comparison with uncoated beads.



\*\*\* Announcing the new DAVID Web Service which allows access to DAVID from various programming languages. [More info...](#) \*\*\*

## Functional Annotation Chart

[Help and Manual](#)

Current Gene List: combined\_david

Current Background: Homo sapiens

5115 DAVID IDs

Sublist	Category	Term	RT	Genes	Count	%	P-Value	Benjamini
<input type="checkbox"/>	KEGG_PATHWAY	<a href="#">Axon guidance</a>	<a href="#">RT</a>	<input type="checkbox"/>	58	1.1	6.5E-7	1.3E-4
<input type="checkbox"/>	KEGG_PATHWAY	<a href="#">MAPK signaling pathway</a>	<a href="#">RT</a>	<input type="checkbox"/>	94	1.8	7.5E-5	7.2E-3
<input type="checkbox"/>	KEGG_PATHWAY	<a href="#">Calcium signaling pathway</a>	<a href="#">RT</a>	<input type="checkbox"/>	64	1.3	4.7E-4	3.0E-2
<input type="checkbox"/>	KEGG_PATHWAY	<a href="#">GnRH signaling pathway</a>	<a href="#">RT</a>	<input type="checkbox"/>	39	0.8	1.2E-3	5.5E-2
<input type="checkbox"/>	KEGG_PATHWAY	<a href="#">Melanogenesis</a>	<a href="#">RT</a>	<input type="checkbox"/>	39	0.8	1.5E-3	5.5E-2
<input type="checkbox"/>	KEGG_PATHWAY	<a href="#">Pathways in cancer</a>	<a href="#">RT</a>	<input type="checkbox"/>	104	2.0	2.3E-3	7.1E-2
<input type="checkbox"/>	KEGG_PATHWAY	<a href="#">Glycerophospholipid metabolism</a>	<a href="#">RT</a>	<input type="checkbox"/>	28	0.5	3.9E-3	1.0E-1
<input type="checkbox"/>	KEGG_PATHWAY	<a href="#">Endocytosis</a>	<a href="#">RT</a>	<input type="checkbox"/>	61	1.2	7.6E-3	1.7E-1
<input type="checkbox"/>	KEGG_PATHWAY	<a href="#">Long-term depression</a>	<a href="#">RT</a>	<input type="checkbox"/>	27	0.5	1.0E-2	2.0E-1
<input type="checkbox"/>	KEGG_PATHWAY	<a href="#">Prostate cancer</a>	<a href="#">RT</a>	<input type="checkbox"/>	33	0.6	1.0E-2	1.8E-1
<input type="checkbox"/>	KEGG_PATHWAY	<a href="#">Insulin signaling pathway</a>	<a href="#">RT</a>	<input type="checkbox"/>	46	0.9	1.3E-2	2.0E-1
<input type="checkbox"/>	KEGG_PATHWAY	<a href="#">Wnt signaling pathway</a>	<a href="#">RT</a>	<input type="checkbox"/>	50	1.0	1.6E-2	2.3E-1
<input type="checkbox"/>	KEGG_PATHWAY	<a href="#">Dilated cardiomyopathy</a>	<a href="#">RT</a>	<input type="checkbox"/>	33	0.6	1.7E-2	2.3E-1
<input type="checkbox"/>	KEGG_PATHWAY	<a href="#">Hedgehog signaling pathway</a>	<a href="#">RT</a>	<input type="checkbox"/>	22	0.4	2.1E-2	2.5E-1
<input type="checkbox"/>	KEGG_PATHWAY	<a href="#">Cell adhesion molecules (CAMs)</a>	<a href="#">RT</a>	<input type="checkbox"/>	44	0.9	2.2E-2	2.5E-1
<input type="checkbox"/>	KEGG_PATHWAY	<a href="#">ErbB signaling pathway</a>	<a href="#">RT</a>	<input type="checkbox"/>	31	0.6	2.4E-2	2.5E-1
<input type="checkbox"/>	KEGG_PATHWAY	<a href="#">Adherens junction</a>	<a href="#">RT</a>	<input type="checkbox"/>	28	0.5	2.5E-2	2.5E-1
<input type="checkbox"/>	KEGG_PATHWAY	<a href="#">Colorectal cancer</a>	<a href="#">RT</a>	<input type="checkbox"/>	30	0.6	2.5E-2	2.4E-1
<input type="checkbox"/>	KEGG_PATHWAY	<a href="#">Vascular smooth muscle contraction</a>	<a href="#">RT</a>	<input type="checkbox"/>	38	0.7	2.6E-2	2.3E-1
<input type="checkbox"/>	KEGG_PATHWAY	<a href="#">Phosphatidylinositol signaling system</a>	<a href="#">RT</a>	<input type="checkbox"/>	27	0.5	2.7E-2	2.3E-1
<input type="checkbox"/>	KEGG_PATHWAY	<a href="#">Basal cell carcinoma</a>	<a href="#">RT</a>	<input type="checkbox"/>	21	0.4	3.4E-2	2.7E-1
<input type="checkbox"/>	KEGG_PATHWAY	<a href="#">Glioma</a>	<a href="#">RT</a>	<input type="checkbox"/>	23	0.4	4.2E-2	3.1E-1
<input type="checkbox"/>	KEGG_PATHWAY	<a href="#">Neurotrophin signaling pathway</a>	<a href="#">RT</a>	<input type="checkbox"/>	40	0.8	4.8E-2	3.4E-1
<input type="checkbox"/>	KEGG_PATHWAY	<a href="#">Gap junction</a>	<a href="#">RT</a>	<input type="checkbox"/>	30	0.6	5.3E-2	3.6E-1

**FIG E2.** The most significant pathways reflected from the predicted gene list of the significant miRNAs using DAVID.



## Functional Annotation Chart

[Help and Manual](#)

Current Gene List: **Input\_Pathway\_Express\_Diff\_25(2)**

Current Background: **Homo sapiens**

83 DAVID IDs

Options

Rerun Using Options

Create Sublist

13 chart records

[Download File](#)

Sublist	Category	Term	RT	Genes	Count	%	P-Value	Benjamini
<input type="checkbox"/>	KEGG_PATHWAY	<a href="#">Systemic lupus erythematosus</a>	RT		8	9.6	3.0E-6	1.7E-4
<input type="checkbox"/>	KEGG_PATHWAY	<a href="#">Viral myocarditis</a>	RT		7	8.4	5.9E-6	1.7E-4
<input type="checkbox"/>	KEGG_PATHWAY	<a href="#">Asthma</a>	RT		5	6.0	3.5E-5	6.8E-4
<input type="checkbox"/>	KEGG_PATHWAY	<a href="#">Allograft rejection</a>	RT		5	6.0	8.4E-5	1.2E-3
<input type="checkbox"/>	KEGG_PATHWAY	<a href="#">Graft-versus-host disease</a>	RT		5	6.0	1.2E-4	1.3E-3
<input type="checkbox"/>	KEGG_PATHWAY	<a href="#">Type I diabetes mellitus</a>	RT		5	6.0	1.6E-4	1.5E-3
<input type="checkbox"/>	KEGG_PATHWAY	<a href="#">Antigen processing and presentation</a>	RT		6	7.2	2.0E-4	1.6E-3
<input type="checkbox"/>	KEGG_PATHWAY	<a href="#">Cell adhesion molecules (CAMs)</a>	RT		7	8.4	2.0E-4	1.5E-3
<input type="checkbox"/>	KEGG_PATHWAY	<a href="#">Intestinal immune network for IgA production</a>	RT		5	6.0	2.9E-4	1.8E-3
<input type="checkbox"/>	KEGG_PATHWAY	<a href="#">Autoimmune thyroid disease</a>	RT		5	6.0	3.3E-4	1.9E-3
<input type="checkbox"/>	KEGG_PATHWAY	<a href="#">Prion diseases</a>	RT		3	3.6	2.2E-2	1.1E-1
<input type="checkbox"/>	KEGG_PATHWAY	<a href="#">Pathogenic Escherichia coli infection</a>	RT		3	3.6	5.5E-2	2.4E-1
<input type="checkbox"/>	KEGG_PATHWAY	<a href="#">Complement and coagulation cascades</a>	RT		3	3.6	7.7E-2	3.0E-1

**FIG E3.** Asthma is reflected as one of the most important pathways from the differentially regulated epithelial genes in asthmatic patients and healthy subjects.

**TABLE E1.** Prioritized miRNAs reflecting differences between groups

SI no.	miRNA	miRbase accession ID	Ct' = 35 - Ct (SD)			Fold change			P value (t test)		
			Healthy subjects	Asthmatic patients	Patients with TB	Asthmatic patients/ healthy subjects	Patients with TB/ healthy subjects	Patients with TB/ asthmatic patients	Healthy subjects-asthmatic patients	Healthy subjects-patients with TB	Asthmatic patients-patients with TB
1	hsa-miR-649	MIMAT0003319	0.8 (1.1)	2.6 (1.2)	7.7 (1.6)	3.4	123.2	35.7	.01	3.49245E-08	1.15165E-06
2	hsa-miR-1264	MIMAT0005791	0.9 (1.3)	2.7 (1.6)	6.9 (1.5)	3.4	64.0	19.0	.05	1.95612E-07	<.001
3	hsa-miR-2861	MIMAT0013802	0.95 (1.3)	3.5 (3.5)	6.6 (1.3)	5.8	50.6	8.7	.05	1.80722E-07	.02
4	hsa-miR-574-5p	MIMAT0004795	1.0 (1.4)	2.8 (1.9)	6.2 (1.2)	3.3	35.3	10.6	.04	5.13377E-07	<.001
5	hsa-miR-421	MIMAT0003339	3.9 (5.9)	7.3 (5.5)	5.5 (NA)	9.8	2.9	0.3	.25	NA	NA
6	hsa-miR-624	MIMAT0003293	3.6 (3.2)	5.7 (4.5)	3.9 (5.6)	4.0	1.2	0.3	.3	.9	.5
7	hsa-miR-453	MIMAT0001630	1.7 (1.3)	0.3 (0.6)	8.6 (1.1)	0.4	118.7	305.8	.03	1.06123E-07	1.7536E-10
8	hsa-miR-4256	MIMAT0016877	4.7 (2.9)	1.7 (2.1)	6.8 (1.1)	0.1	4.2	17.5	.02	.07	1.12E-05
9	hsa-miR-516a-5p	MIMAT0004770	7.9 (4.2)	4.2 (3.0)	2.7 (5.1)	0.1	0.02	1.0	.09	.07	.5
10	hsa-miR-1913	MIMAT0007888	0.61 (0.9)	0.20 (1.82)	16.7 (0.3)	2.7	68,662.2	92,681.9	.3	.1	.8
11	hsa-miR-556-5p	MIMAT0003220	3.1 (2.8)	0.7 (1.2)	0 (0)	0.2	0.1	0.9	.03	.01	.1

The prioritized miRNA (healthy subjects vs asthmatic patients) along with their miRBase accession IDs, average counts along with their SDs, and fold changes in samples from healthy subjects, asthmatic patients, and patients with tuberculosis are shown. The figure also shows the *P* values for the same. The Bonferroni adjusted threshold for significance was .0001 and was only reached in samples from patients with tuberculosis.

*TB*, Tuberculosis.

**TABLE E2.** miRNnome versus transcriptome

<b>Common genes between the targets for the downregulated miRNAs in exhaled breath and the upregulated genes in nasal transcriptome</b>	<b>Common genes between the targets for the upregulated miRNAs in exhaled breath and the downregulated genes in nasal transcriptome</b>
<i>C2orf43</i>	<i>PAX7</i>
<i>HLA-DPB1</i>	<i>TTC4</i>
<i>ZNF518A</i>	<i>SUMF1</i>
<i>NAV2</i>	<i>GFOD1</i>
<i>BRD3</i>	<i>NAGPA</i>
	<i>TOMM22</i>
	<i>SLCO2A1</i>
	<i>TRAPPC1</i>
	<i>RYBP</i>
	<i>KLHL35</i>

The common gene targets between the miRNAs differentially regulated in EBC and the differentially regulated genes in the nasal epithelium are shown. Predicted mRNA targets of upregulated miRNAs were downregulated in nasal transcriptome (eg, *SLCO2A1* and *PAX7*) and *vice versa* (eg, *HLA-DPB1* and *NAV2*). This requires validation and is a preliminary observation.